# Supporting information

## Investigation of Li-excess Manganese Oxide Spinel Structure for Electrochemical Water Oxidation Catalysis

**Deepika Tavar[a,b], Kamlesh[a,b], Satya Prakash[a,b], Mohammad Ashiq[a,b], Pradeep Singh[c], Pankaj Raizada[c], R.K. Sharma[d], A.K.Srivastava[a,b], Archana Singh[a,b,*],**

[a]Academy of Scientific & Innovative Research (AcSIR), Ghaziabad 201002, India

[b]CSIR– Advanced Material and Processes Research Institute, Bhopal 462026, India

[c]School of Chemistry, Faculty of Basic Sciences, Shoolini University, Solan (HP), India—173229

[d]Raja Ramanna Research Center, Indore, India

*archanasingh@ampri.res.in

**Table S1.** Rietveld refined Structural parameter of $Li_4Mn_5O_{12}$, $LiMn_2O_4$, λ-$MnO_2$

| | Atoms | Site | x | y | z |
|---|---|---|---|---|---|
| λ$MnO_2$ | Mn1 | 16d | 0.5 | 0.5 | 0.5 |
| | O1 | 32e | 0.26339 | 0.26339 | 0.26339 |
| | a=8.0568, cell volume=522.983, Rp=31.2%, Rwp=19.3%, GOF=1.61 | | | | |
| $LiMn_2O_4$ | Li1 | 8a | 0.125 | 0.125 | 0.125 |
| | Mn1 | 16d | 0.5 | 0.5 | 0.5 |
| | O1 | 32e | 0.264 | 0.264 | 0.264 |
| | a=8.1851, cell volume=548.367, Rp=15.04%, Rwp=22%, GOF=2.13 | | | | |
| $Li_4Mn_5O_{12}$ | Li | 16d | 0.0 | 0.0 | 0.0 |
| | L1 | 8a | 0.37500 | 0.37500 | 0.37500 |
| | Mn | 16d | 0.0 | 0.0 | 0.0 |
| | Mn | 8a | 0.37500 | 0.37500 | 0.37500 |
| | O | 32e | 0.24680 | 0.24680 | 0.24680 |
| | a=8.1377, cell volume=538.896, Rp=5.07%, Rwp=2.73%, GOF=1.78 | | | | |

**Table S2.** ICP-MS analysis result for the $Li_4Mn_5O_{12}$, $LiMn_2O_4$. The amounts of Li and Mn shown below are in gram obtained for 1 g of $Li_4Mn_5O_{12}$, $LiMn_2O_4$.

| Li/Mn(molar ratio) | Prepared using γ-MnOOH in $LiNO_3$ medium $Li_4Mn_5O_{12}$ | | Prepared using γ-MnOOH in LiOH medium $LiMn_2O_4$ | |
|---|---|---|---|---|
| 1:1 | Li | Mn | Li | Mn |
| | 0.047 | 0.682 | 0.051 | 0.7931 |

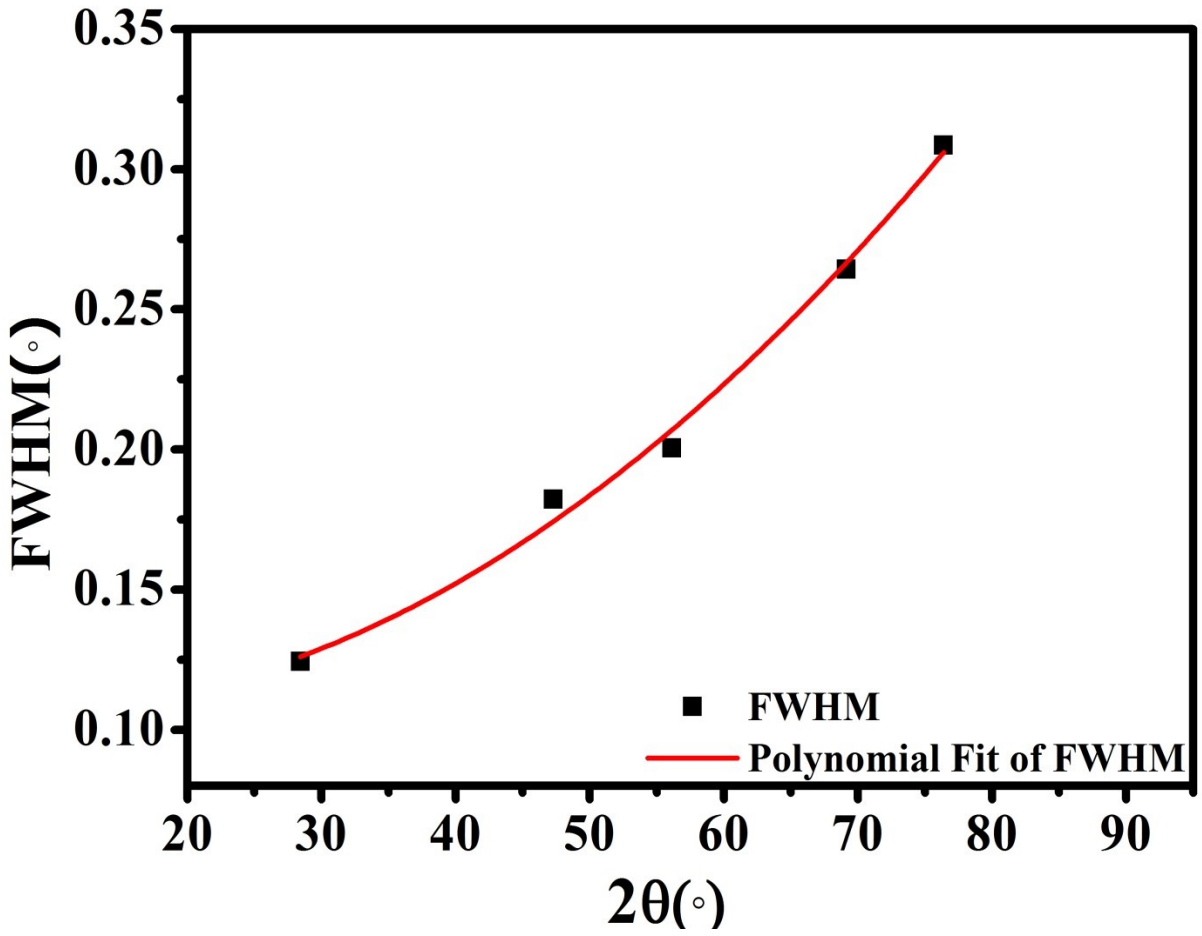


**Fig. S0.** Instrumental broadening against 2θ for standard Silicon powder

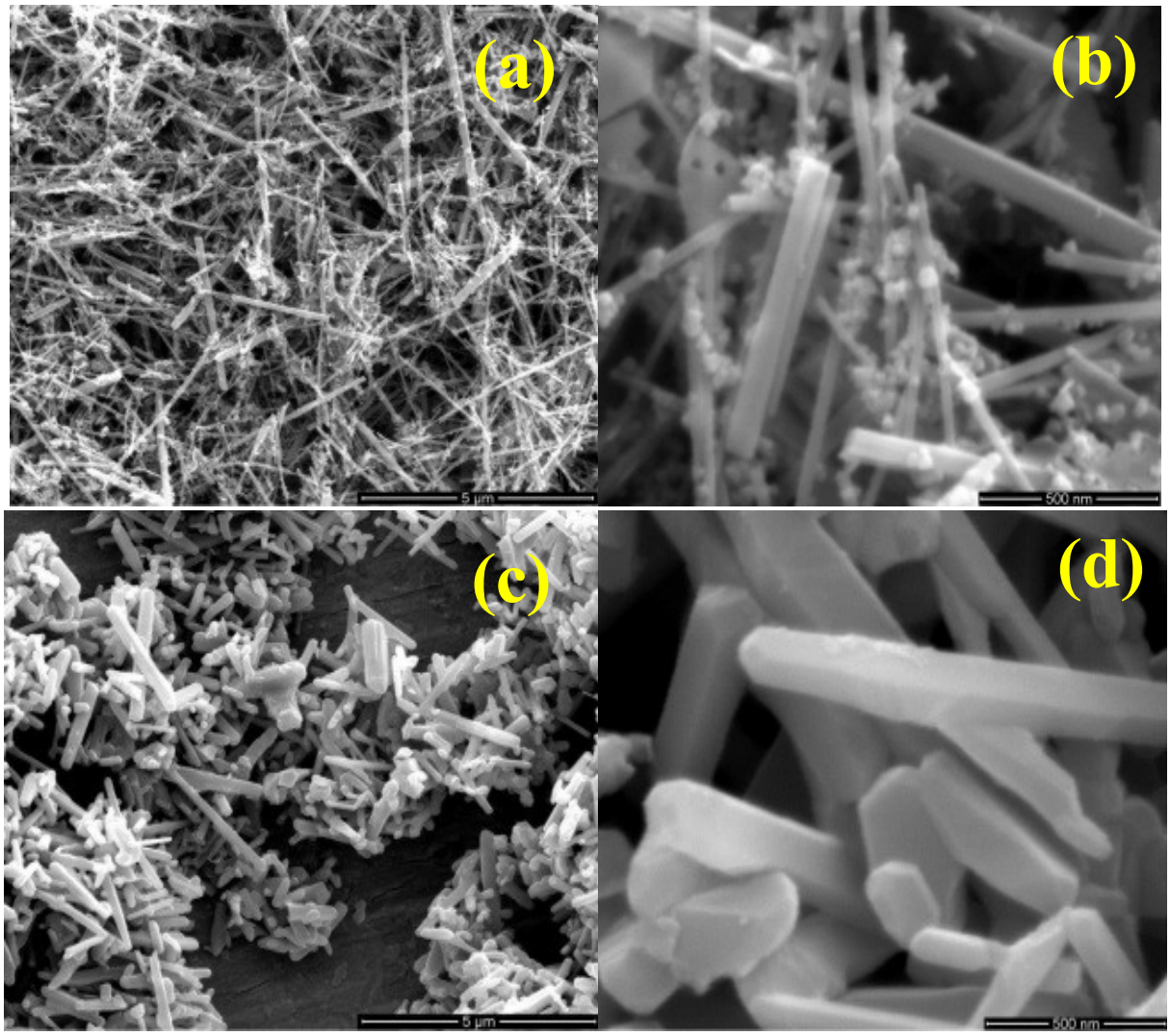


**Fig. S1.** SEM images of (a) $Li_4Mn_5O_{12}$ at 5µm, (b) $Li_4Mn_5O_{12}$ at 500nm, (c) $LiMn_2O_4$ at 5µm and (d) $LiMn_2O_4$ at 500 nm.

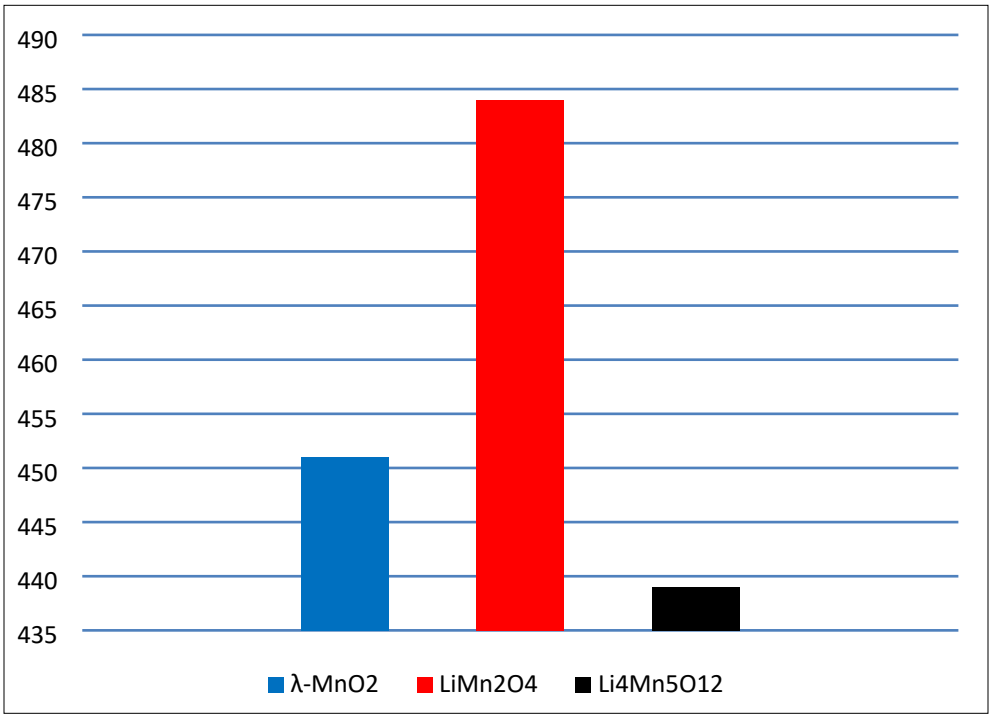


**Fig. S2.** Overpotential at Current density 5mA/cm$^2$

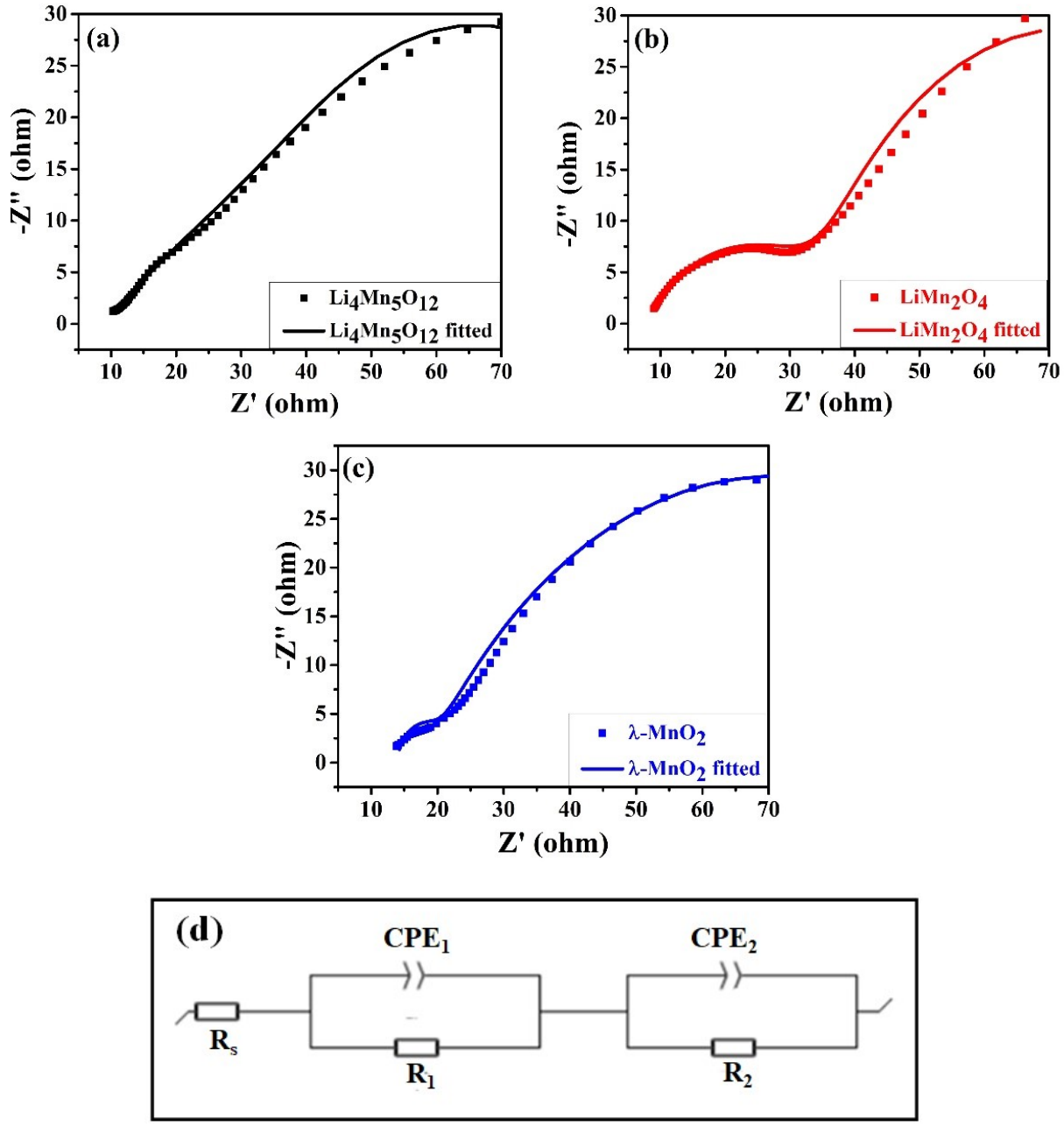


**Fig. S3.** Nyquist plots of (a) $Li_4Mn_5O_{12}$, (b) $LiMn_2O_4$, (c) λ-$MnO_2$ and (d) equivalent circuit.

**Table S3.** XPS Mn2p peak data of $Li_4Mn_5O_{12}$, $LiMn_2O_4$ and λ-$MnO_2$ before testing

| Compound | Binding energy position (eV) | | Cation distribution | | Mn valence |
|---|---|---|---|---|---|
| | $Mn^{4+}$ | $Mn^{3+}$ | $Mn^{4+}$ (%) | $Mn^{3+}$ (%) | |
| $Li_4Mn_5O_{12}$ | 642.8 | 642.0 | 84.95% | 15.05% | +3.84 |
| $LiMn_2O_4$ | 642.2 | 641.2 | 50.24% | 49.76% | +3.5 |
| λ-$MnO_2$ | 642.2 | 641.9 | 87.14% | 12.86% | +3.84 |

**Table S4.** XPS Mn2p peak data of $Li_4Mn_5O_{12}$ after testing

| Compound | Binding energy position (eV) | | Cation distribution | | Mn valence |
|---|---|---|---|---|---|
| | $Mn^{4+}$ | $Mn^{3+}$ | $Mn^{4+}$ (%) | $Mn^{3+}$ (%) | |
| $Li_4Mn_5O_{12}$ | 641.8 | 640.78 | 91.78% | 8.22 | +3.91 |

**Table S5.** XPS peak fitting results of $O1_S$ core levels of $Li_4Mn_5O_{12}$, $LiMn_2O_4$ and λ-$MnO_2$ before testing.

| Spinel oxide | $O^{2-}$ [%] | $O_2^{2-}/O^-$ [%] | $OH^-$ [%] | $H_2O$ [%] |
|---|---|---|---|---|
| $Li_4Mn_5O_{12}$ | 23.43 | 50.06 | 24.09 | 2.43 |
| $LiMn_2O_4$ | 25.87 | 15.83 | 53.74 | 4.56 |
| λ-$MnO_2$ | 6.20 | 32.33 | 37.89 | 23.58 |

**Table S6.** XPS peak fitting results of $O1_S$ core levels of $Li_4Mn_5O_{12}$ after testing

| Spinel oxide | $O^{2-}$ [%] | $O_2^{2-}/O^-$ [%] | $OH^-$ [%] | $H_2O$ [%] |
|---|---|---|---|---|
| $Li_4Mn_5O_{12}$ | 13.66 | 53.40 | 25.27 | 7.67 |

**Table S7**: Comparison of Turn over frequency (TOF) number for various Mn-O based catalyst (mol $O_2$/s/mol)

| Compound | TOF ($s^{-1}$) | pH | BET ($m^2\ g^{-1}$) | Ref |
|---|---|---|---|---|
| α-$MnO_2$ | $1\times10^{-5}$ | 7 | 62 | [1] |
| $\lambda$-$MnO_2$ (HT) | $5\times10^{-6}$ | 7 | - | [2] |
| $\lambda$-$MnO_2$ (LT) | $3\times10^{-5}$ | 7 | - | [2] |
| δ-$MnO_2$ | $2\times10^{-5}$ | 7 | 96 | [3] |
| $MnO_x$ (amorphous) | $5.5\times10^{-5}$ | 7.2 | 88 | [4] |
| MnO | $2\times10^{-5}$ | 7 | 11 | [5] |
| $Mn_2O_3$ (bixbyite) | $3.7\times10^{-4}$ | 7 | 16.27 | [6] |
| $Mn_3O_4$ | $3\times10^{-4}$ | 7 | 14 | [4] |
| δ-$MnO_2$-$Mn_3O_4$ nanocomposite($MnO_x$-2) | $9.3\times10^{-4}$ | 5.8 | 112 | [3] |
| $K_{0.16}MnO_{1.97}\cdot0.14H_2O$ (cryptomelane) | $5.3\times10^{-5}$ | 5-6 | 140 | [4] |
| $LiMn_2O_4$ (spinel) | LOD* | 7 | 24.5 | [6] |

*LOD = 0.05 nmol O2 s−1

## References


[1] D. Hong, Y. Yamada, A. Nomura, S. Fukuzumi, Catalytic activity of NiMnO 3 for visible light-driven and electrochemical water oxidation, Physical Chemistry Chemical Physics, 15 (2013) 19125-19128.
[2] D.M. Robinson, Y.B. Go, M. Greenblatt, G.C. Dismukes, Water oxidation by λ-MnO2: catalysis by the cubical Mn4O4 subcluster obtained by delithiation of spinel LiMn2O4, Journal of the American Chemical Society, 132 (2010) 11467-11469.
[3] Z. Geng, Y. Wang, J. Liu, G. Li, L. Li, K. Huang, L. Yuan, S. Feng, δ-MnO2–Mn3O4 nanocomposite for photochemical water oxidation: Active structure stabilized in the interface, ACS Applied Materials & Interfaces, 8 (2016) 27825-27831.
[4] A. Iyer, J. Del-Pilar, C.K. King'ondu, E. Kissel, H.F. Garces, H. Huang, A.M. El-Sawy, P.K. Dutta, S.L. Suib, Water oxidation catalysis using amorphous manganese oxides, octahedral molecular sieves (OMS-2), and octahedral layered (OL-1) manganese oxide structures, The Journal of Physical Chemistry C, 116 (2012) 6474-6483.
[5] P.W. Menezes, A. Indra, P. Littlewood, M. Schwarze, C. Göbel, R. Schomäcker, M. Driess, Nanostructured manganese oxides as highly active water oxidation catalysts: a boost from manganese precursor chemistry, ChemSusChem, 7 (2014) 2202-2211.

[6] D.M. Robinson, Y.B. Go, M. Mui, G. Gardner, Z. Zhang, D. Mastrogiovanni, E. Garfunkel, J. Li, M. Greenblatt, G.C. Dismukes, Photochemical water oxidation by crystalline polymorphs of manganese oxides: structural requirements for catalysis, Journal of the American chemical Society, 135 (2013) 3494-3501.